

A SURVEY FOR NEW MEMBERS OF TAURUS WITH THE SPITZER SPACE TELESCOPE

K. L. LUHMAN¹, B. A. WHITNEY², M. R. MEADE³, B. L. BABLER³, R. INDEBETOUW⁴, S. BRACKER³, AND E. B. CHURCHWELL³

Draft version October 4, 2018

ABSTRACT

We present the results of a search for new members of the Taurus star-forming region using the Infrared Array Camera (IRAC) aboard the *Spitzer Space Telescope*. With IRAC images of 29.7 deg² of Taurus at 3.6, 4.5, 5.8, and 8.0 μm , we have identified sources with red mid-infrared colors indicative of disk-bearing objects and have obtained optical and infrared spectra of 23 of these candidate members. Through this work, we have discovered 13 new members of Taurus, two of which have spectral types later than M6 and thus are likely to be brown dwarfs according to the theoretical evolutionary models of Chabrier and Baraffe. This survey indicates that the previous census of Taurus has a completeness of $\sim 80\%$ for members with disks. The new members that we have found do not significantly modify the previously measured distributions of Taurus members as a function of position, mass, and extinction. For instance, we find no evidence for a population of highly reddened brown dwarfs ($A_K \sim 2$) that has been missed by previous optical and near-infrared surveys, which suggests that brown dwarf disks are not significantly more flared than disks around stars. In addition to the new members, we also present IRAC photometry for the 149 previously known members that appear within this survey, which includes 27 objects later than M6.

Subject headings: infrared: stars — stars: evolution — stars: formation — stars: low-mass, brown dwarfs — stars: luminosity function, mass function — stars: pre-main sequence

1. INTRODUCTION

As one of the nearest sites of active star formation ($d = 140$ pc), the Taurus complex of dark clouds has long been a popular laboratory for studies of the birth of stars and planets. A fundamental prerequisite for most observations of Taurus is a census of its stellar content. Over the decades, a variety of methods have been employed to identify members of Taurus, including objective prism spectroscopy of H α (Joy 1946, 1949; Briceño et al. 1993, 1999), X-ray imaging with the *Einstein Observatory* (Feigelson et al. 1987; Walter et al. 1988) and the *Röntgen Satellite* (Strom & Strom 1994; Neuhäuser et al. 1995; Wichmann et al. 1996; Briceño et al. 1999), proper motion measurements (Jones & Herbig 1979; Hartmann et al. 1991; Gomez et al. 1992), near- and mid-infrared (IR) photometry from ground-based telescopes (Gomez et al. 1994; Itoh et al. 1996; Luhman & Rieke 1998) and the *Infrared Astronomical Satellite (IRAS)* (Beichman et al. 1986; Kenyon et al. 1990, 1994), and wide-field optical and near-IR imaging (Briceño et al. 1998, 2002; Luhman 2000, 2004b, 2006; Luhman et al. 2003a; Martín et al. 2001; Guieu et al. 2006). The census of known members of Taurus has steadily grown (Cohen & Kuhl 1979; Herbig & Bell 1988; Kenyon & Hartmann 1995) and now contains more than 300 stars and brown dwarfs.

The *Spitzer Space Telescope* (Werner et al. 2004) of-

fers a combination of sensitivity and large field of view that is unprecedented for a mid-IR telescope, making it uniquely suited for finding disk-bearing objects down to low masses ($M \sim 0.01 M_{\odot}$), through high levels of extinction ($A_V \sim 100$), and across large areas of sky ($\theta \sim 10^\circ$). To take advantage of this capability, we have used archival *Spitzer* images encompassing 29.7 deg² of Taurus to perform a search for new members of the region. In this paper, we present the collection and analysis of the *Spitzer* data (§ 2), the identification of candidate members with these data (§ 3), the spectroscopy and classification of these candidates (§ 4), an evaluation of the completeness of this survey and previous ones (§ 5), and the implications of our updated census for the distribution of Taurus members as a function of position, mass, and extinction and the implications of our mid-IR photometric catalog for the frequency of disks in Taurus (§ 6).

2. ANALYSIS OF SPITZER DATA

To search for new members of Taurus, we used unpublished archival images at 3.6, 4.5, 5.8, and 8.0 μm that were obtained with the Infrared Array Camera (IRAC; Fazio et al. 2004) aboard the *Spitzer Space Telescope* during the General Observer program 3584 by D. Padgett. The plate scale and field of view of IRAC are $1''.2$ and $5'.2 \times 5'.2$, respectively. The camera produces images with FWHM = $1''.6$ – $1''.9$ from 3.6 to 8.0 μm . The IRAC data for Taurus were collected between 2005 February 20 and 27 (UT). The images were obtained in 16 adjacent maps, each of which contained a mosaic of pointings separated by $290''$ and aligned with the array axes. At each cell in the map, images were obtained in the 12 s high dynamic range (HDR) mode, which provided one 0.4 s exposure and one 10.4 s exposure. Each of the 16 maps was observed twice. These observations encompassed a

¹ Department of Astronomy and Astrophysics, The Pennsylvania State University, University Park, PA 16802; kluhman@astro.psu.edu.

² Space Science Institute, 4750 Walnut Street, Suite 205, Boulder, CO 80301.

³ Department of Astronomy, The University of Wisconsin, 475 North Charter Street, Madison, WI 53706.

⁴ Department of Astronomy, University of Virginia, P.O. Box 3818, Charlottesville, VA 22903-0818.

total area of 29.7 deg². The boundaries of the imaged fields are indicated in the map of Taurus in Figure 1.

The IRAC images were processed with the S11.4.0 pipeline from the *Spitzer* Science Center and the pipeline for the Galactic Legacy Infrared Mid-Plane Survey Extraordinaire (GLIMPSE, Benjamin et al. 2003) after it was modified to enable the processing of HDR frames. Sources were extracted from individual frames using a modified version of DAOPHOT (Stetson 1987)⁵. Before the photometry was measured, image defects were corrected and saturated stars were masked. The image defects included column pulldown and muxbleed for 3.6 and 4.5 μm and banding for 5.8 and 8.0 μm (Hora et al. 2004). We did not mask cosmic rays because overmasking of cosmic rays can modify stellar fluxes. An array-location-dependent photometric correction was applied to the IRAC photometry as specified by the *Spitzer* Science Center⁶. The sources were merged across observations and wavelengths using the *Spitzer* Science Center bandmerger, as modified by GLIMPSE. At this step, the IRAC sources were merged with near-IR sources from the Point Source Catalog of the Two-Micron All-Sky Survey (2MASS, Skrutskie et al. 2006). To prevent cosmic rays from being falsely included in our source lists, we required detections of each source in at least two adjacent IRAC bands with a signal-to-noise ratio (SNR) greater than 5 in at least one and two bands for 0.4 and 10.4 sec, respectively. These criteria were developed through analysis of color-color and color-magnitude diagrams and comparison of 0.4 to 10.4 sec data for the Taurus data in this work and observations of the Large Magellanic Cloud by Meixner et al. (2006). Even if the source is reliable, the photometry in all bands may not be. Therefore, for both the 0.4 and 10.4 sec data, we rejected the flux in a band if $\text{SNR} \leq 5$ in the combined measurement from the two exposures for that band. For the 10.4 sec data, we excluded photometry brighter than 9.5, 9.0, 6.5, and 6.5 mag at 3.6, 4.5, 5.8, and 8.0 μm , respectively. For the 0.4 sec data, we flag as upper limits the magnitudes brighter than 6.0, 5.5, 3.0, and 3.0 mag, respectively. When merging the catalogs for the short and long exposures, we matched a pair of sources if the separation was less than 0".7. For these objects, we compared the short and long exposure data at a given band and adopted the measurement with the smallest error. The list of IRAC sources, which we refer to as the Taurus IRAC Point Source Archive (or "the Archive"), contains $\sim 450,000$ sources and will be available to the public⁷.

We used the calibration from Reach et al. (2005), which differs slightly from the calibration applied to previous IRAC measurements in Taurus by Hartmann et al. (2005). After adjusting the data from Hartmann et al. (2005) to the calibration from Reach et al. (2005) and comparing photometry for ~ 40 sources appearing in both studies, we find that the average photometry for each band agrees between the two studies to within $\sim 2\%$.

3. SELECTION OF CANDIDATE MEMBERS OF TAURUS

⁵ For more details concerning the photometry routines and GLIMPSE pipeline processing, see the GLIMPSE documents at <http://www.astro.wisc.edu/glimpse/docs.html>.

⁶ <http://ssc.spitzer.caltech.edu/irac/locationcolor>

⁷ <http://www.astro.wisc.edu/glimpse/Taurus>

To develop criteria for identifying sources in the Archive that could be new members of Taurus, we examined the colors exhibited by previously known members appearing within the IRAC survey. According to published membership lists for Taurus (§ 1), 149 resolved, previously known members are encompassed by the IRAC images. One of these members, the protostar IRAS 04368+2557, is not in the Archive because it is extended and thus was missed by our automated software for finding point sources. Although the binary IT Tau is resolved by the IRAC images, the software identified only one source. We measured separate photometry for IT Tau A and B by inputting the known positions of the two objects into the pipeline and included these data in the Archive. Among IT Tau A and B and the remaining 146 members in the Archive, 118 objects have photometric uncertainties less than 0.1 mag in all four IRAC bands. These members are plotted in a diagram of $[3.6] - [4.5]$ versus $[5.8] - [8.0]$ in Figure 2. As demonstrated in the IRAC survey of known Taurus members by Hartmann et al. (2005), different areas in this diagram correspond to different classes of mid-IR spectral energy distributions (Lada & Wilking 1984). Stars that lack significant amounts of circumstellar dust (class III) reside near the origin in Figure 2 while stars with disks (class II) and stars with both disks and infalling envelopes (class 0 and I) have progressively redder mid-IR colors. The neutral colors of diskless members of Taurus make them indistinguishable from field stars in IRAC data. However, the other classes are more easily separated from most contaminants. In particular, Hartmann et al. (2005) showed that most of the disk-bearing objects in their sample exhibited colors of $[3.6] - [4.5] > 0.15$ and $[5.8] - [8.0] > 0.3$. Therefore, to identify candidate class I and II members of Taurus in the new IRAC survey, we applied these criteria to the $\sim 27,000$ sources in the Archive with photometric errors less than 0.1 mag in all four bands, which are shown in Figure 2. We selected for spectroscopy 20 candidates that satisfy these color criteria and that appear within the range of magnitudes encompassed by previously known members ($[3.6] \lesssim 13$, Figure 3). The star HD 283751 exhibits excess emission in the IRAC bands, but was classified as a background Be star by Jones & Herbig (1979), and thus has been excluded from this work.

We also searched for candidate members of Taurus among the IRAC sources that have errors less than 0.1 mag in only three bands. The absence of an accurate measurement for one of the four bands was typically because of saturation (usually at 3.6 μm), contamination by a cosmic ray, or simply low signal-to-noise (usually 5.8 or 8.0 μm). To identify candidate class I and II objects among these IRAC sources, we analyzed all possible IRAC color-color diagrams containing three bands in the same manner as $[3.6] - [4.5]$ versus $[5.8] - [8.0]$. In this way, we selected one candidate from each of $[3.6] - [4.5]$ versus $[4.5] - [8.0]$, $[3.6] - [5.8]$ versus $[5.8] - [8.0]$, and $[4.5] - [5.8]$ versus $[5.8] - [8.0]$. The diagram of $[3.6] - [4.5]$ versus $[4.5] - [5.8]$ reveals ~ 30 candidates, but they are excluded as promising candidates because they are significantly fainter than expected at 8 μm relative to the other bands for sources with disks.

Spectroscopic observations of the above 23 candidates

are described in the next section. In § 4, we classify 13 candidates as Taurus members and 10 candidates as nonmembers.

4. SPECTROSCOPY OF CANDIDATES

4.1. Observations

We performed optical and near-IR spectroscopy on the 23 candidate Taurus members that were selected in the previous section using the Marcario Low-Resolution Spectrograph (LRS) on the Hobby-Eberly Telescope (HET), the Low Dispersion Survey Spectrograph (LDSS-3) on the Magellan II Telescope, and SpeX on the Infrared Telescope Facility (IRTF). Table 1 summarizes the observing runs and instrument configurations for these data. In Tables 2 and 3, we indicate the night on which each object was observed. The procedures for the collection and reduction of the optical spectra were similar to those described by Luhman (2004b). The IR spectra obtained with SpeX (Rayner et al. 2003) were reduced with the Spextool package (Cushing, Vacca, & Rayner 2004) and corrected for telluric absorption with the method from Vacca et al. (2003).

4.2. Spectral Classification

To determine if the candidates in our spectroscopic sample are members of Taurus rather than background sources, particularly red galaxies, and to measure their spectral types, we applied optical and IR classification methods that are identical to those employed in the recent survey for new Taurus members by Luhman (2006). The diagnostics of youth (and thus membership in Taurus) consist of emission lines, IR excess emission, gravity-sensitive spectral features, and reddening. For the new members of Taurus, we measured spectral types from the absorption bands of VO and TiO ($\lambda < 1.3 \mu\text{m}$) and H₂O ($\lambda > 1 \mu\text{m}$) using averages of spectra of dwarfs and giants as the spectroscopic standards at optical wavelengths (Luhman 1999) and optically-classified young objects as the standards at IR wavelengths. Based on the optical and IR spectra, we classify 13 candidates as members of Taurus. Seven of the remaining 10 candidates have emission lines that are indicative of active galaxies at redshifts of $z=0.07-0.22$. The final three candidates, 2MASS J04233697+2526284, J04252936+2654238, and J04385618+2342078, lack both detectable stellar features and emission lines from galaxies. The spectra of class I stars can appear featureless because of continuum veiling from dust, but these three objects are much bluer than expected for embedded stars of this kind. It is possible that the presence of edge-on disks could explain both the blue near-IR colors and red mid-IR colors. However, for the purposes of this work, we classify them as nonmembers. The 2MASS identifications and 2MASS and IRAC photometry for the members and nonmembers are provided in Tables 2 and 3, respectively. For each of the new members, we also include our spectral classification and the evidence of membership in Taurus. The spectra of the new members are presented in order of spectral type in Figs. 4 and 5. To facilitate the comparison of these spectra, they have been corrected for reddening (Luhman 2004a; Luhman et al. 2005a). The positions of the new members are indicated in the map of Taurus in Figure 1.

4.3. Comments on Individual Sources

Three of the new members were previously identified as candidate members of Taurus through detections of *K*-band excess emission. Those near-IR data were collected by Itoh et al. (1996) (ITG) and the astrometry and photometry for the candidates, ITG 1, 15, and 40, were reported by Itoh et al. (1999). ITG 15 also was identified as a near-IR source by Tamura et al. (1996) and ITG 40 is probably star 32 from the near-IR survey of Gomez et al. (1994). Itoh et al. (2002) reported confirmation of the membership of ITG 15 and 40 through *K*-band spectroscopy. However, they did not identify any specific evidence of youth or membership in their data. Among the new members, ITG 1 exhibits the reddest IRAC colors and is probably a class I object based on its location in Figure 2 (Hartmann et al. 2005). One of the new members, 2MASS J04224786+2645530, was previously detected by IRAS. Finally, we note that the optical and IR spectra of 2MASS 04390525+2337450 contain many strong emission lines, including H α , He I, and [O I], [O II], [N II], and [S II], which are indicative of an actively accreting classical T Tauri star with a jet or an outflow.

5. SURVEY COMPLETENESS

We now evaluate the completeness of both our survey and previous surveys in Taurus. As mentioned in § 3, 116 of the 146 previously known Taurus members in the IRAC survey fields that were automatically identified as point sources have photometric uncertainties less than 0.1 mag in all four IRAC bands, and thus satisfy the photometric criteria that we applied to the Archive in constructing the diagram of $[3.6] - [4.5]$ versus $[5.8] - [8.0]$. An additional 12 of the known members have accurate photometry in three bands, so they satisfy the criteria for the three-band color-color diagrams with which we selected candidates. The remaining 18 known members lack good photometry in three bands because they are saturated (4), in the field of view of only two filters (13), or surrounded by extended emission (1). If we exclude the members along the edges of the maps with only 2-band coverage and consider only the area with 4-band coverage, then the color-color diagrams employed in selecting candidates contain 128/136 (94%) of the previously known members (class 0 through III). This percentage represents an estimate of the completeness of our photometric sample of class I and II candidates for the same range of magnitudes and extinctions exhibited by previously known members. Because we did not obtain spectra of all of these candidates, our spectroscopic completeness is lower. However, as shown in the diagram of $[3.6]$ versus $[3.6] - [8.0]$ in Figure 3, the ranges of colors and magnitudes exhibited by previously known Taurus members contain only ~ 8 remaining class I and II candidates that have not been observed spectroscopically. Because this survey targeted only class I and II objects, and roughly half of Taurus members fall in these classes, it is likely that another 10-20 class III members remain undiscovered in our survey field.

We can quantify the limits in mass and extinction for which our survey is complete (for classes I and II) by examining the diagram of $[3.6]$ versus $[3.6] - [8.0]$ in Figure 3, where we show the known members of Taurus and the remaining sources from Figure 2 that have red colors but lack spectroscopy. We include in Figure 3 the photo-

metric completeness limit of these data, which was taken to be the value of $[8.0]$ above which the number of sources as a function of $[8.0]$ stops rising. This limit is computed from $[8.0]$ because it is the least sensitive IRAC band for the ranges of colors in question. As demonstrated in Figure 3, the extinction limit of our survey for class II members ($0.5 \lesssim [3.6] - [8.0] \lesssim 2.2$) is very high, ranging from $A_K \sim 10$ for $2 M_\odot$ ($[3.6] \sim 6$) to $A_K \sim 2$ for $0.02 M_\odot$ ($[3.6] \sim 12.5$). For instance, if the known substellar class II members of Taurus were reddened by $A_K = 2$, our survey would still detect most of them. The completeness also is high for the ranges of colors and magnitudes expected for class I objects at stellar masses ($[3.6] - [8.0] \gtrsim 2.2$, $[3.6] < 11$), where there are only two candidates that lack spectroscopy. One of these objects, 2MASS 04293209+2430597, is directly within a filament of known members and thus is a promising candidate class I source. At the fainter levels expected for class I brown dwarfs, there remain a large number of candidates (~ 500) that have not been observed spectroscopically, most of which are probably galaxies based on their uniform spatial distribution. In addition to these class I candidates, Figures 2 and 3 contain several objects that lack spectroscopy and have colors and magnitudes ($0.5 \lesssim [3.6] - [8.0] \lesssim 1.5$, $[3.6] > 13$) that are indicative of class II brown dwarfs at very low masses ($M \sim 0.01 M_\odot$).

We can use the new members that we have found to assess the completeness of previous surveys. The recent study by Luhman (2006) considered an area of 225 deg^2 that encompasses the entire field imaged by IRAC. The search criteria in that survey were designed for spectral types later than M6, and two of the new members in this work are later than this threshold, 2MASS 04242090+2630511 (M6.5) and 2MASS 04335245+2612548 (M8.5). They were missed by Luhman (2006) because the former is slightly too blue in $I2 - K_s$ ⁸ and the latter has 2MASS uncertainties that are too large. The fact that two objects of this kind were not found by Luhman (2006) is consistent with the level of completeness estimated in that study ($\sim 75\%$). The survey of a smaller area of Taurus by Luhman (2004b) encompassed three of our new members, ITG 1, 15, and 40. ITG 40 (M3.5) was not found because it is earlier than the spectral type limit of $\geq M4$ considered in that search. ITG 15 (M5) is later than this limit, but it was missed because it is 0.07 mag bluer than the $I - K_s$ threshold that was adopted for selecting candidates. ITG 1 was not identified as a candidate because it was below the sequence of Taurus members in the color-magnitude diagrams from Luhman (2004b), which is common for class I objects because they are often observed in scattered light. Incompleteness for scattered-light sources was acknowledged by Luhman (2004b). The IRAC survey also overlaps significantly with the recent optical survey by Guieu et al. (2006). Ten of our new members are located within the area considered in that study. Four of these objects were not found because they are earlier than the range of spectral types that was searched ($\geq M4$). ITG 1 was probably missed in the same manner described for Luhman (2004b). The remaining five new members are within the range of spectral types and

extinctions searched by Guieu et al. (2006), and consist of 2MASS 04230607+2801194 (M6), 04242090+2630511 (M6.5), 04335245+2612548 (M8.5), 04362151+2351165 (M5.25), and ITG 15 (M5). As discussed by Luhman (2006), the completeness of the survey by Guieu et al. (2006) is lower than they reported, and these overlooked objects further demonstrate this.

The level of completeness of previous membership surveys of Taurus at spectral types of M2-M6 has been unknown because of a possible gap between the faint limits of the wide-field X-ray and objective prism surveys and the bright limits of deep optical broad-band imaging surveys (Luhman 2004b, 2006). Indeed, 9 of the 11 new members with measured spectral types are in this range of spectral types, as illustrated by the distributions of spectral types in Figure 6 for previously known members within the IRAC survey and for new members. The color criteria in Figure 2 that we used to select class I and II candidates are satisfied by 12 new members, 65 previously known members, and 8 objects that lack spectroscopy and appear within the ranges of colors and magnitudes of previously known members, which implies a completeness of $\sim 76\text{-}84\%$ for the sum total of all previous surveys across the portion of Taurus imaged by IRAC.

6. IMPLICATIONS OF SURVEY

Because of its sensitivity and large areal coverage, our survey of Taurus has direct implications for the distributions of Taurus members as a function of position, mass, and extinction. As demonstrated in the map of Taurus in Figure 1, the spatial distribution of the new class I and II sources is similar to that of the previously known members in classes 0 through III. Among only class II sources, most of the new members are clustered near areas of high extinction in the same manner as the previously known members, while three of the new sources in the southeast part of the survey area are relatively far from dark clouds. However, in general, the previous surveys have provided an accurate measurement of the distribution of class II objects in Taurus. In the portion of our survey that overlaps with areas imaged by Briceño et al. (2002) and Luhman (2004b), we have found only a few new members. As a result, the measurements of initial mass functions presented in those studies do not require significant revisions and accurately reflect the Taurus stellar population. The extinction limits of our search for class II members of Taurus are very high, and yet the extinctions of the new members are similar to those of the previously known ones. Thus, as with position and mass, the previously measured distribution of members as a function of extinction also appears to be representative of Taurus. In particular, some models of brown dwarf disks have suggested that these disks might have higher scale heights than disks around stars, which would result in higher average extinctions for class II brown dwarfs relative to class II stars if the gas and dust are well-mixed (Walker et al. 2004). However, we do not find a population of brown dwarfs that are more highly reddened than the previously known ones that were discovered in optical and near-IR surveys, which suggests that the disks around brown dwarfs do not have higher scale heights, or if they do, that the dust has settled. Overall, the measured distributions of Taurus members

⁸ $I2$ is the second epoch near-IR magnitude in the USNO-B1.0 Catalog (Monet et al. 2003).

as a function of position, mass, and extinction are not changed significantly by our survey.

In addition to identifying new members, the IRAC images also provide mid-IR photometry for nearly half of the previously known members of Taurus. For several members, a measurement in a given band is unavailable in the original Archive because a detection was present in only one of the two exposures for that band. In these cases, we manually inspected the images to determine if the measurement from the one image was sufficient. In this way, we recovered photometry for LkCa 21, J1-665, CFHT 20, FZ Tau, PSC 04158+2805, and 2MASS 04242090+2630511 in [4.5] and GO Tau and IRAS 04239+2436 in [8.0]. In Table 4, we present IRAC measurements for 144 known members of Taurus that are within the IRAC fields, excluding five class I members with extended emission. For the latter objects, we measured photometry for apertures across a range of radii, which is provided in Table 5. These measurements have uncertainties of ~ 0.1 mag. Only one of these class I sources, IRAS 04248+2612, has photometry in the Archive that satisfied the criteria used in constructing Figure 2. Thus, it is the only one appearing in that diagram, and it is plotted with the default photometry from the Archive rather than the measurements in Table 5. We note that the colors of the class I sources in Table 5 vary with aperture size and are distributed all over color-color space, including inside the class II region, which has been predicted by models (Whitney et al. 2003) and observed in previous IRAC measurements in Taurus (Hartmann et al. 2005).

With the IRAC measurements, we can measure the frequency of disks among stars and brown dwarfs in Taurus. For this measurement, we must exclude the new members that we have found in this work because they were identified through the presence of disk emission. These new members cannot be included in a disk fraction measurement unless a new survey is performed that encompasses these objects among its identified members and that is unbiased in terms of disks. In addition, we consider only the 118 previously known members that have photometric uncertainties less than 0.1 mag in all four IRAC bands. Based on these data, which are shown in Figure 2, we measure disk fractions of $57/93=61 \pm 8\%$ for the stars ($\leq M6$) and $10/25=40 \pm 13\%$ for the brown dwarfs ($>M6$)⁹. This measurement for the stars in Taurus is higher than the disk fractions for stellar members of IC 348 ($33 \pm 4\%$) and Chamaeleon I ($45 \pm 7\%$) that were measured from IRAC data by Luhman et al. (2005b), which is consistent with the younger age of Taurus ($\tau \sim 1$ Myr, Briceño et al. 2002; Luhman et al. 2003a) relative to these two clusters ($\tau \sim 2$ Myr, Luhman et al. 2003b; Luhman 2004a). Unlike IC 348 and Chamaeleon I, the disk fraction of brown dwarfs in Taurus is lower than that of the stars, but this difference has only marginal statistical significance and may be the result of the incompleteness of the current census of Taurus for class I brown dwarfs.

7. CONCLUSIONS

⁹ The hydrogen burning mass limit at ages of 0.5-3 Myr corresponds to a spectral type of $\sim M6.25$ according to the models of Baraffe et al. (1998) and Chabrier et al. (2000) and the temperature scale of Luhman et al. (2003b).

We have presented the results of a mid-IR imaging survey of 29.7 deg^2 of the Taurus star-forming region that was performed with IRAC aboard the *Spitzer Space Telescope*. We used these data to search for new members of Taurus by identifying objects with colors indicative of circumstellar disks. Through spectroscopy of 23 of these candidates, we have discovered 13 new members. One of these objects appears to be a class I source based on its IRAC colors, while two of the new members have spectral types later than M6 and thus are likely to be brown dwarfs. The number of new members found in this survey indicates that the previous census of Taurus exhibits a completeness of $\sim 80\%$ for class I and II sources. Meanwhile, by considering the number of previously known members of Taurus that we have recovered, we estimate that our survey has a completeness of $\sim 94\%$ for class I and II members. This completeness extends to high levels of extinction, ranging from $A_K \sim 2-10$ for $M \sim 0.02-2 M_\odot$. If brown dwarf disks are more flared than disks around stars, than the average extinction toward brown dwarfs should be higher than toward stars, but we have found no evidence of this in our survey. The new members that we have found do not significantly alter the distributions of Taurus members as a function of position, mass, and extinction that have been measured in previous membership surveys.

In addition to performing a search for new members of Taurus, we have also measured mid-IR photometry for the 149 previously known members of Taurus within the IRAC survey, which comprises nearly half of the known membership. With these data, we have measured disk fractions of $61 \pm 8\%$ and $40 \pm 13\%$ for the stellar ($\leq M6$) and substellar ($>M6$) members of Taurus. The disk fraction for stars in Taurus is higher than the fraction for stellar members of IC 348 and Chamaeleon I, which is consistent with the slightly younger age of Taurus implied by Hertzsprung-Russell diagrams of these populations. Meanwhile, the difference in disk fractions for stars and brown dwarfs in Taurus has only marginal statistical significance and may be a reflection of the incompleteness for class I brown dwarfs in surveys of this region to date. Indeed, ~ 500 candidate members of Taurus from this IRAC survey remain unobserved with spectroscopy, most of which would be class I brown dwarfs if confirmed, although a vast majority are probably red galaxies.

K. L. was supported by grant NAG5-11627 from the NASA Long-Term Space Astrophysics program. This work made use of the GLIMPSE data processing pipeline which was supported by the Spitzer Space Telescope Legacy program through NASA contracts 1224653 and 1224988. This work is based in part on observations made with the *Spitzer Space Telescope*, which is operated by the Jet Propulsion Laboratory, California Institute of Technology under a contract with NASA. This work also is based on observations performed at the IRTF and the HET. The IRTF is operated by the University of Hawaii under Cooperative Agreement no. NCC 5-538 with the National Aeronautics and Space Administration, Office of Space Science, Planetary Astronomy Program. The HET is a joint project of the University of Texas at Austin, the Pennsylvania State University, Stanford University, Ludwig-Maximilians-Universität München,

and Georg-August-Universität Göttingen. The HET is named in honor of its principal benefactors, William P. Hobby and Robert E. Eberly. The Marcario Low-Resolution Spectrograph at HET is named for Mike Marcario of High Lonesome Optics, who fabricated several optics for the instrument but died before its completion; it is a joint project of the Hobby-Eberly Telescope partnership and the Instituto de Astronomía de la Univer-

sidad Nacional Autónoma de México. This publication makes use of data products from the Two Micron All Sky Survey, which is a joint project of the University of Massachusetts and the Infrared Processing and Analysis Center/California Institute of Technology, funded by the National Aeronautics and Space Administration and the National Science Foundation.

REFERENCES

- Baraffe, I., Chabrier, G., Allard, F., & Hauschildt, P. H. 1998, *A&A*, 337, 403
- Beichman, C. A., Myers, P. C., Emerson, J. P., Harris, S., Mathieu, R., Benson, P. J., & Jennings, R. E. 1986, *ApJ*, 307, 337
- Benjamin, R. A., et al. 2003, *PASP*, 115, 953
- Briceño, C., Calvet, N., Gomez, M., Hartmann, L. W., Kenyon, S. J., & Whitney, B. A. 1993, *PASP*, 105, 686
- Briceño, C., Hartmann, L., Stauffer, J., & Martín, E. L., 1998, *AJ*, 115, 2074
- Briceño, C., Calvet, N., Kenyon, S., & Hartmann, L. 1999, *AJ*, 118, 1354
- Briceño, C., Luhman, K. L., Hartmann, L., Stauffer, J. R., & Kirkpatrick, J. D. 2002, *ApJ*, 580, 317
- Chabrier, G., Baraffe, I. Allard, F., & Hauschildt, P. H. 2000, *ApJ*, 542, 464
- Cohen, M., & Kuhl, L. V. 1979, *ApJS*, 41, 743
- Cushing, M. C., Vacca, W. D., & Rayner, J. T. 2004, *PASP*, 116, 362
- Dobashi, K., Uehara, H., Kandori, R., Sakurai, T., Kaiden, M., Umamoto, T., & Sato, F. 2005, *PASJ*, 57, 1
- Fazio, G. G., et al. 2004, *ApJS*, 154, 10
- Feigelson, E. D., Jackson, J. M., Mathieu, R. D., Myers, P. C., & Walter, F. M. 1987, *AJ*, 94, 1251
- Gomez, M., Jones, B. F., Hartmann, L., Kenyon, S. J., Stauffer, J. R., Hewett, R., & Reid, I. N. 1992, *AJ*, 104, 762
- Gomez, M., Kenyon, S. J., & Hartmann, L. 1994, *AJ*, 107, 1850
- Guieu, S., Dougados, C., Monin, J.-L., Magnier, E. & Martín, E. L. 2006, *A&A*, 446, 485
- Hartmann, L., Stauffer, J. R., Kenyon, S. J., & Jones, B. F. 1991, *AJ*, 101, 1050
- Hartmann, L., et al. 2005, *ApJ*, 629, 881
- Herbig, G. H., & Bell, K. R. 1988, *Lick Obs. Bull. Ser.*, No. 1111
- Hora, J. L., et al. 2004, *SPIE*, 5487, 77
- Indebetouw, R., et al. 2005, *ApJ*, 619, 9311
- Itoh, Y., Tamura, M., & Gatley, I. 1996, *ApJ*, 465, L129
- Itoh, Y., Tamura, M., & Nakajima, T. 1999, *AJ*, 117, 1471
- Itoh, Y., Tamura, M., & Tokunaga, A. T. 2002, *PASJ*, 54, 561
- Jones, B. F., & Herbig, G. H. 1979, *AJ*, 84, 1872
- Joy, A. H. 1946, *PASP*, 58, 244
- Joy, A. H. 1949, *ApJ*, 110, 424
- Kenyon, S. J., & Hartmann, L. 1995, *ApJS*, 101, 117
- Kenyon, S. J., Hartmann, L. W., Strom, K. M., & Strom, S. E. 1990, *AJ*, 99, 869
- Kenyon, S. J., Gomez, M., Marzke, R. O., & Hartmann, L. 1994, *AJ*, 108, 251
- Lada, C. J., & Wilking, B. A. 1984, *ApJ*, 287, 610
- Luhman, K. L. 1999, *ApJ*, 525, 466
- Luhman, K. L. 2000, *ApJ*, 544, 1044
- Luhman, K. L. 2004a, *ApJ*, 602, 816
- Luhman, K. L. 2004b, *ApJ*, 617, 1216
- Luhman, K. L. 2006, *ApJ*, in press
- Luhman, K. L., & Rieke, G. H. 1998, *ApJ*, 497, 354
- Luhman, K. L., Briceño, C., Stauffer, J. R., Hartmann, L., Barrado y Navascués, D., & Nelson, C. 2003a, *ApJ*, 590, 348
- Luhman, K. L., Stauffer, J. R., Muench, A. A., Rieke, G. H., Lada, E. A., Bouvier, J., & Lada, C. J. 2003b, *ApJ*, 593, 1093
- Luhman, K. L., Lada, E. A., Muench, A. A., & Elston, R. J. 2005a, *ApJ*, 618, 810
- Luhman, K. L., et al. 2005b, *ApJ*, 631, L69
- Martín, E. L., Dougados, C., Magnier, E., Ménard, F., Magazzù, A., Cuilandre, J.-C., & Delfosse, X. 2001, *ApJ*, 561, L195
- Meixner, M., et al. 2006, *AJ*, submitted
- Monet, D. G., et al. 2003, *AJ*, 125, 984
- Neuhäuser, R., Sterzik, M. F., Schmitt, J. H. M. M., Wichmann, R., & Krautter, J. 1995, *A&A*, 297, 391
- Rayner, J. T., et al. 2003, *PASP*, 115, 362
- Reach, W. T., et al. 2005, *PASP*, 117, 978
- Skrutskie, M., et al. 2006, *AJ*, 131, 1163
- Stetson, P. 1987, *PASP*, 99, 191
- Strom, K. M., & Strom, S. E. 1994, *ApJ*, 424, 237
- Tamura, M., Ohashi, N., Hirano, N., Itoh, Y., & Moriarty-Schieven, G. H. 1996, *AJ*, 112, 2076
- Vacca, W. D., Cushing, M. C., & Rayner J. T., 2003, *PASP*, 115, 389
- Walker, C., Wood, K., Lada, C. J., Robitaille, T., Bjorkman, J. E., & Whitney, B. 2004, *MNRAS*, 351, 607
- Walter, F. M., Brown, A., Mathieu, R. D., Myers, P. C., & Vrba, F. J. 1988, *AJ*, 96, 297
- Werner, M. W., et al. 2004, *ApJS*, 154, 1
- Whitney, B. A., Wood, K., Bjorkman, J. E., & Cohen, M. 2003, *ApJ*, 598, 1079
- Wichmann, R., et al. 1996, *A&A*, 312, 439

TABLE 1
OBSERVING LOG

Night	Date	Telescope + Instrument	Disperser	λ (μm)	$\lambda/\Delta\lambda$
1	2005 Dec 12	IRTF + SpeX	prism	0.8-2.5	100
2	2005 Dec 13	IRTF + SpeX	prism	0.8-2.5	100
3	2005 Dec 14	IRTF + SpeX	prism	0.8-2.5	100
4	2005 Dec 20	HET + LRS	G3 grism	0.63-0.91	1100
5	2005 Dec 23	HET + LRS	G3 grism	0.63-0.91	1100
6	2005 Dec 25	HET + LRS	G3 grism	0.63-0.91	1100
7	2005 Dec 26	HET + LRS	G3 grism	0.63-0.91	1100
8	2006 Feb 9	Magellan II + LDSS-3	VPH red grism	0.68-1.1	1300
9	2006 Feb 10	Magellan II + LDSS-3	VPH red grism	0.58-1	1300

TABLE 2
NEW MEMBERS OF TAURUS

2MASS ^a	Spectral Type ^b	Membership Evidence ^c	$J - H^a$	$H - K_s^a$	K_s^a	[3.6]	[4.5]	[5.8]	[8.0]
J04224786+2645530 ^d	M1	e, A_V , ex	1.44	0.86	9.29	8.17 \pm 0.06	7.45 \pm 0.06	6.99 \pm 0.03	6.26 \pm 0.02
J04230607+2801194	M6.5(IR), M6(op)	NaK, e, H_2O , ex	0.63	0.41	11.20	10.56 \pm 0.03	10.27 \pm 0.05	9.89 \pm 0.04	9.35 \pm 0.03
J04231822+2641156	M3.5	A_V , ex	1.64	0.84	10.18	9.42 \pm 0.05	9.08 \pm 0.04	8.70 \pm 0.03	8.08 \pm 0.03
J04242090+2630511	M7(IR), M6.5(op)	e, H_2O , ex, NaK	0.68	0.38	12.43	11.80 \pm 0.05	11.42 \pm 0.10	10.99 \pm 0.04	10.33 \pm 0.03
J04293606+2435556	M3	A_V , ex	1.39	0.73	8.66	7.91 \pm 0.04	7.67 \pm 0.06	7.40 \pm 0.04	6.96 \pm 0.03
J04335245+2612548	M8.5	A_V , H_2O , ex	1.21	0.60	13.99	13.08 \pm 0.05	12.56 \pm 0.07	12.17 \pm 0.05	11.39 \pm 0.04
J04362151+2351165	M5.25	NaK, ex	0.63	0.29	12.24	11.73 \pm 0.04	11.46 \pm 0.05	11.06 \pm 0.04	10.50 \pm 0.03
J04375670+2546229 ^e	?	e, ex	0.87	0.56	12.70	11.95 \pm 0.06	11.31 \pm 0.06	10.70 \pm 0.03	9.75 \pm 0.03
J04390525+2337450	?	e, ex	1.08	0.75	11.55	10.51 \pm 0.05	10.10 \pm 0.04	9.68 \pm 0.03	8.93 \pm 0.02
J04393364+2359212	M4.75(IR), M5(op)	NaK, H_2O , ex	0.76	0.53	10.28	9.57 \pm 0.03	9.17 \pm 0.04	8.76 \pm 0.02	7.91 \pm 0.03
J04394488+2601527 ^f	M4.75(IR), M5(op)	NaK, e, A_V , H_2O , ex	1.12	0.57	8.95	8.37 \pm 0.04	8.06 \pm 0.05	7.67 \pm 0.04	7.01 \pm 0.03
J04400067+2358211	M6.5(IR), M6(op)	NaK, e, H_2O , ex	0.56	0.39	11.48	10.84 \pm 0.06	10.60 \pm 0.06	10.29 \pm 0.04	9.66 \pm 0.02
J04412464+2543530 ^g	M3.5	A_V , ex	3.18	1.78	11.75	10.35 \pm 0.04	9.77 \pm 0.04	9.35 \pm 0.03	8.84 \pm 0.03

^a2MASS Point Source Catalog.^bUncertainties are ± 0.25 and ± 0.5 subclass for the optical and IR types from this work, respectively, unless noted otherwise.^cMembership in Taurus is indicated by $A_V \gtrsim 1$ and a position above the main sequence for the distance of Taurus (" A_V "), strong emission lines ("e"), Na I a strengths intermediate between those of dwarfs and giants ("NaK"), IR excess emission ("ex"), or the shape of the gravity-sensitive steam bands (" H_2O ").^dIRAS 04196+2638.^eITG 1.^fITG 15.^gITG 40.TABLE 3
NONMEMBERS

2MASS ^a	$J - H^a$	$H - K_s^a$	K_s^a	[3.6]	[4.5]	[5.8]	[8.0]	Night
J04233697+2526284	1.28	0.97	14.51	13.11 \pm 0.06	12.17 \pm 0.07	11.22 \pm 0.04	10.08 \pm 0.03	3
J04252936+2654238	1.23	0.22	15.85	...	13.20 \pm 0.07	12.65 \pm 0.07	11.89 \pm 0.05	4
J04253556+2457398	0.88	0.96	14.00	12.70 \pm 0.06	11.98 \pm 0.05	11.29 \pm 0.03	10.04 \pm 0.03	3
J04260493+2302201	1.06	0.95	14.61	13.61 \pm 0.04	12.82 \pm 0.05	12.09 \pm 0.04	10.68 \pm 0.03	2
J04275447+2424145	0.90	0.99	14.15	12.68 \pm 0.07	11.79 \pm 0.06	11.06 \pm 0.05	10.07 \pm 0.02	3
J04340188+2319066	1.02	0.93	14.38	12.54 \pm 0.05	11.88 \pm 0.06	11.11 \pm 0.04	10.21 \pm 0.03	3
J04350207+2331415	0.93	0.55	14.21	13.05 \pm 0.06	12.52 \pm 0.08	11.86 \pm 0.04	10.90 \pm 0.03	2,5
J04362486+2621473	1.36	1.13	13.89	12.55 \pm 0.06	11.83 \pm 0.05	11.15 \pm 0.04	10.33 \pm 0.03	2
J04385618+2342078	0.53	0.31	14.91	14.74 \pm 0.06	14.53 \pm 0.06	14.34 \pm 0.19	13.28 \pm 0.07	8
J04443086+2614092	1.05	1.05	13.54	11.42 \pm 0.04	10.33 \pm 0.04	9.44 \pm 0.03	8.35 \pm 0.02	2,5

^a2MASS Point Source Catalog.

TABLE 4
PREVIOUSLY KNOWN MEMBERS OF TAURUS IN SPITZER SURVEY

2MASS ^a	Other Name	$J - H^a$	$H - K_s^a$	K_s^a	[3.6]	[4.5]	[5.8]	[8.0]
J04173372+2820468	CY Tau	0.86	0.37	8.60	7.85±0.03	7.56±0.06	7.22±0.03	6.69±0.02
J04174955+2813318	KPNO 10	0.75	0.35	10.79	10.75±0.03	10.32±0.03	9.78±0.02	8.84±0.02
J04174965+2829362	V410 X-ray 1	1.29	0.65	9.08	...	7.75±0.05	...	6.43±0.03
J04180796+2826036	V410 X-ray 3	0.73	0.37	10.45	9.99±0.06	9.89±0.05	9.77±0.03	9.75±0.03
J04181710+2828419	V410 Anon 13	1.29	0.70	10.96	...	9.82±0.06	...	8.81±0.03
J04182239+2824375	V410 Anon 24	2.89	1.53	10.73	9.80±0.04	9.46±0.05	9.27±0.03	9.28±0.03
J04182909+2826191	V410 Anon 25	3.27	1.70	9.94	8.87±0.04	8.53±0.05	8.35±0.03	8.34±0.03
J04183030+2743208	KPNO 11	0.61	0.26	11.01	10.63±0.04	10.53±0.05	10.44±0.03	10.48±0.04
J04183110+2827162	V410 Tau A+B+C	0.66	0.16	7.63	7.26±0.04	7.32±0.04	7.22±0.03	7.21±0.02
J04183112+2816290	DD Tau A+B	1.15	0.80	7.88	6.41±0.03	5.73±0.03	5.21±0.03	4.42±0.02
J04183158+2816585	CZ Tau A+B	0.74	0.41	9.36	8.39±0.04	7.55±0.05	6.53±0.02	4.98±0.02
J04183203+2831153	PSC 04154+2823	2.82	2.09	10.27	...	6.98±0.04	...	5.47±0.03
J04183444+2830302	V410 X-ray 2	3.06	1.49	9.21	...	8.04±0.05	...	7.46±0.03
J04184023+2824245	V410 X-ray 4	2.68	1.28	9.69	8.81±0.04	8.56±0.05	8.38±0.03	8.42±0.03
J04184061+2819155	V892 Tau	1.73	1.23	5.79	<5.04	...	3.58±0.03	...
J04184133+2827250	LR1	3.30	1.87	11.05	9.48±0.07	8.79±0.05	8.33±0.03	7.91±0.03
J04184250+2818498	V410 X-ray 7	1.83	0.84	9.26	8.65±0.05	8.53±0.05	8.39±0.04	8.33±0.08
J04184505+2820528	V410 Anon 20	2.99	1.48	11.93	10.94±0.04	10.70±0.07	10.50±0.04	10.48±0.04
J04184703+2820073	Hubble 4	0.92	0.34	7.29	7.03±0.04	7.00±0.04	6.91±0.03	6.92±0.02
J04185115+2814332	KPNO 2	0.68	0.49	12.75	12.21±0.07	12.07±0.04	11.99±0.05	11.86±0.07
J04185147+2820264	CoKu Tau/1	1.38	0.52	10.97	10.28±0.04	8.90±0.05	7.62±0.02	5.77±0.02
J04185813+2812234	PSC 04158+2805	1.43	1.17	11.18	9.12±0.04	8.47±0.09	7.76±0.03	6.78±0.03
J04190110+2819420	V410 X-ray 6	0.93	0.47	9.13	8.79±0.05	8.63±0.07	8.49±0.04	8.24±0.02
J04190126+2802487	KPNO 12	0.82	0.56	14.93	13.93±0.06	13.54±0.05	13.17±0.10	12.63±0.06
J04190197+2822332	V410 X-ray 5a	1.20	0.63	10.15	9.59±0.05	9.47±0.06	9.37±0.03	9.36±0.03
J04191281+2829330	FQ Tau A+B	0.79	0.39	9.31	...	8.34±0.05	...	7.39±0.02
J04192625+2826142	V819 Tau	0.85	0.22	8.42	8.14±0.03	8.13±0.06	8.05±0.03	8.00±0.03
J04193545+2827218	FR Tau	0.58	0.40	9.97	9.34±0.04	8.79±0.06	8.17±0.02	7.21±0.03
J04194127+2749484	LkCa 7A+B	0.74	0.12	8.26	7.95±0.04	7.98±0.07	7.95±0.03	7.94±0.03
J04194148+2716070	IRAS 04166+2706	1.30	0.79	12.62	11.28±0.06	10.35±0.05	9.86±0.03	9.29±0.03
J04195844+2709570	IRAS 04169+2702	...	2.57	11.58	8.40±0.05	...	6.28±0.03	...
J04215740+2826355	RY Tau	1.03	0.73	5.39	3.48±0.03	<2.78
J04215884+2818066	HD 283572	0.41	0.14	6.87	6.77±0.04	6.80±0.05	6.72±0.04	6.74±0.03
J04220313+2825389	LkCa 21	0.79	0.22	8.45	8.14±0.03	8.15±0.090	8.10±0.03	8.05±0.03
J04230776+2805573	IRAS 04200+2759	1.58	1.19	10.41	8.37±0.04	7.77±0.05	7.21±0.03	6.42±0.02
J04242646+2649503	CFHT 9	0.69	0.43	11.76	11.13±0.04	10.85±0.05	10.49±0.03	9.80±0.03
J04244457+2610141	IRAS 04216+2603	1.04	0.70	9.05	7.95±0.07	7.49±0.04	6.99±0.03	6.30±0.03
J04244506+2701447	J1-4423	0.63	0.26	10.46	10.14±0.06	10.06±0.04	10.02±0.04	10.06±0.03
J04245708+2711565	IP Tau	0.89	0.54	8.35	7.70±0.06	7.44±0.05	7.18±0.03	6.49±0.03
J04251767+2617504	J1-4872A	1.06	-0.07	8.54	8.93±0.06	8.87±0.07	8.84±0.04	8.88±0.03
J04251767+2617504	J1-4872B	8.35±0.04	8.32±0.06	8.19±0.04	8.21±0.03
J04262939+2624137	KPNO 3	0.82	0.42	12.08	11.38±0.05	10.90±0.05	10.48±0.04	9.67±0.02
J04265352+2606543	FV Tau A+B	1.59	0.88	7.44	6.22±0.03	5.64±0.04	5.22±0.02	4.52±0.03
J04265440+2606510	FV Tau/c A+B	1.31	0.62	8.87	7.89±0.04	7.48±0.04	6.99±0.03	6.26±0.02
J04265629+2443353	IRAS 04239+2436	3.40	2.36	9.99	7.55±0.05	6.23±0.04	5.32±0.03	4.51±0.04
J04265732+2606284	KPNO 13	1.11	0.59	9.58	8.67±0.04	8.32±0.06	7.90±0.03	7.34±0.02
J04270266+2605304	DG Tau B	8.73±0.06	6.99±0.06	5.76±0.04	4.72±0.03
J04270280+2542223	DF Tau A+B	0.91	0.52	6.73	<5.84	<5.37	5.01±0.02	4.42±0.03
J04270469+2606163	DG Tau	0.97	0.73	6.99	<5.73	...	4.46±0.03	3.56±0.03
J04272799+2612052	KPNO 4	0.97	0.74	13.28	12.49±0.04	12.34±0.06	12.20±0.06	12.11±0.06
J04274538+2357243	CFHT 15	0.70	0.55	13.69	13.17±0.03	13.06±0.07	12.95±0.06	12.86±0.10
J04284263+2714039	...	1.04	0.61	10.46	9.68±0.04	9.45±0.06	9.23±0.03	8.80±0.02
J04290068+2755033	...	0.69	0.47	12.85	12.33±0.06	11.96±0.05	11.57±0.04	10.87±0.03
J04290498+2649073	IRAS 04260+2642	1.65	1.14	11.88	10.01±0.04	9.23±0.07	8.72±0.05	8.03±0.03
J04292071+2633406	J1-507	0.73	0.30	8.79	8.51±0.04	8.47±0.06	8.36±0.03	8.42±0.03
J04292165+2701259	IRAS 04263+2654, CFHT 18	1.30	0.77	8.72	8.06±0.04	7.63±0.06	7.24±0.02	6.65±0.02
J04292373+2433002	GV Tau A+B	1.96	1.53	8.05	<2.43	...
J04292971+2616532	FW Tau A+B	0.66	0.29	9.39	8.96±0.04	8.91±0.07	8.89±0.04	8.85±0.03
J04293008+2439550	IRAS 04264+2433	1.75	0.85	11.13	10.18±0.09	9.39±0.05	8.54±0.03	6.68±0.02
J04294155+2632582	DH Tau	0.94	0.65	8.18	7.58±0.06	7.26±0.06	7.13±0.03	6.80±0.02
J04294247+2632493	DI Tau A+B	0.72	0.21	8.39	8.20±0.04	8.20±0.06	8.10±0.04	8.11±0.03
J04294568+2630468	KPNO 5	0.72	0.38	11.54	11.00±0.06	10.90±0.05	10.84±0.04	10.79±0.04
J04295156+2606448	IQ Tau	1.00	0.64	7.78	6.67±0.06	6.31±0.05	6.00±0.03	5.48±0.03
J04295950+2433078	CFHT 20	1.15	0.73	9.81	8.97±0.05	8.60±0.07	8.29±0.03	7.81±0.03
J04300724+2608207	KPNO 6	0.80	0.51	13.69	13.07±0.06	12.74±0.06	12.36±0.08	11.59±0.07
J04302365+2359129	CFHT 16	0.72	0.55	13.70	13.15±0.05	13.10±0.06	12.95±0.09	12.83±0.09
J04302961+2426450	FX Tau A+B	0.99	0.47	7.92	6.92±0.06	6.80±0.06	6.61±0.03	5.93±0.03
J04304425+2601244	DK Tau A+B	0.96	0.66	7.10	<5.76	5.67±0.09	5.55±0.05	4.82±0.03
J04305028+2300088	IRAS 04278+2253	1.74	1.18	5.86	3.21±0.03	...
J04305137+2442222	ZZ Tau	0.80	0.25	8.44	8.01±0.06	7.85±0.06	7.53±0.03	6.91±0.02
J04305171+2441475	ZZ Tau IRS	1.41	1.12	10.31	8.06±0.06	7.32±0.06	6.62±0.03	5.76±0.03
J04305718+2556394	KPNO 7	0.69	0.56	13.27	12.54±0.04	12.23±0.03	11.89±0.05	11.24±0.02
J04311444+2710179	JH 56	0.67	0.24	8.79	8.74±0.05	8.67±0.06	8.64±0.03	8.57±0.03
J04311907+2335047	...	0.79	0.52	12.20	11.69±0.04	11.48±0.06	11.45±0.05	11.38±0.04
J04312382+2410529	V927 Tau A+B	0.67	0.29	8.77	8.48±0.04	8.43±0.06	8.36±0.03	8.37±0.02
J04312669+2703188	CFHT 13	0.86	0.52	13.45	12.79±0.05	12.70±0.04	12.58±0.06	12.66±0.05
J04315056+2424180	HK Tau A+B	1.20	0.66	8.59	7.57±0.04	7.23±0.04	7.00±0.03	6.59±0.02
J04315844+2543299	J1-665	0.76	0.27	9.56	9.28±0.03	9.24±0.11	9.19±0.03	9.19±0.03
J04320329+2528078	...	0.61	0.39	10.72	10.26±0.06	10.16±0.05	10.07±0.04	10.05±0.03
J04321540+2428507	Hor. 6.13	1.02	1.22	8.10	6.20±0.05	5.78±0.05	5.43±0.03	4.83±0.03

TABLE 5
MEMBERS OF TAURUS WITH EXTENDED EMISSION

2MASS ^a	IRAS	Radius (")	[3.6]	[4.5]	[5.8]	[8.0]
04275730+2619183	04248+2612	4	9.71	9.04	8.33	7.25
		6	9.51	8.89	8.22	7.10
		13	9.29	8.72	8.09	7.01
		26	9.09	8.57	7.92	6.92
04331650+2253204	04302+2247	4	9.97	...	9.57	...
		6	9.80	...	9.41	...
		13	9.63	...	9.26	...
		26	9.49	...	9.09	...
04353539+2408194	04325+2402	4	9.80	9.15	8.98	8.59
		6	9.54	8.92	8.77	8.37
		13	9.16	8.60	8.45	8.15
		26	8.94	8.42	8.23	8.05
04391389+2553208	04361+2547	4	8.04	7.10	6.51	4.97
		6	7.95	7.01	6.43	4.85
		13	7.80	6.88	6.34	4.76
		26	7.66	6.76	6.21	4.70
...	04368+2557	35	7.57	6.77	6.11	4.66
		4	12.70	10.74	9.74	9.47
		6	11.89	10.16	9.25	9.02
		13	10.48	9.13	8.40	8.33
		26	9.32	8.22	7.59	7.68
		60	8.33	7.44	6.91	7.41
		100	8.07	7.28	6.60	7.23

^a2MASS Point Source Catalog.

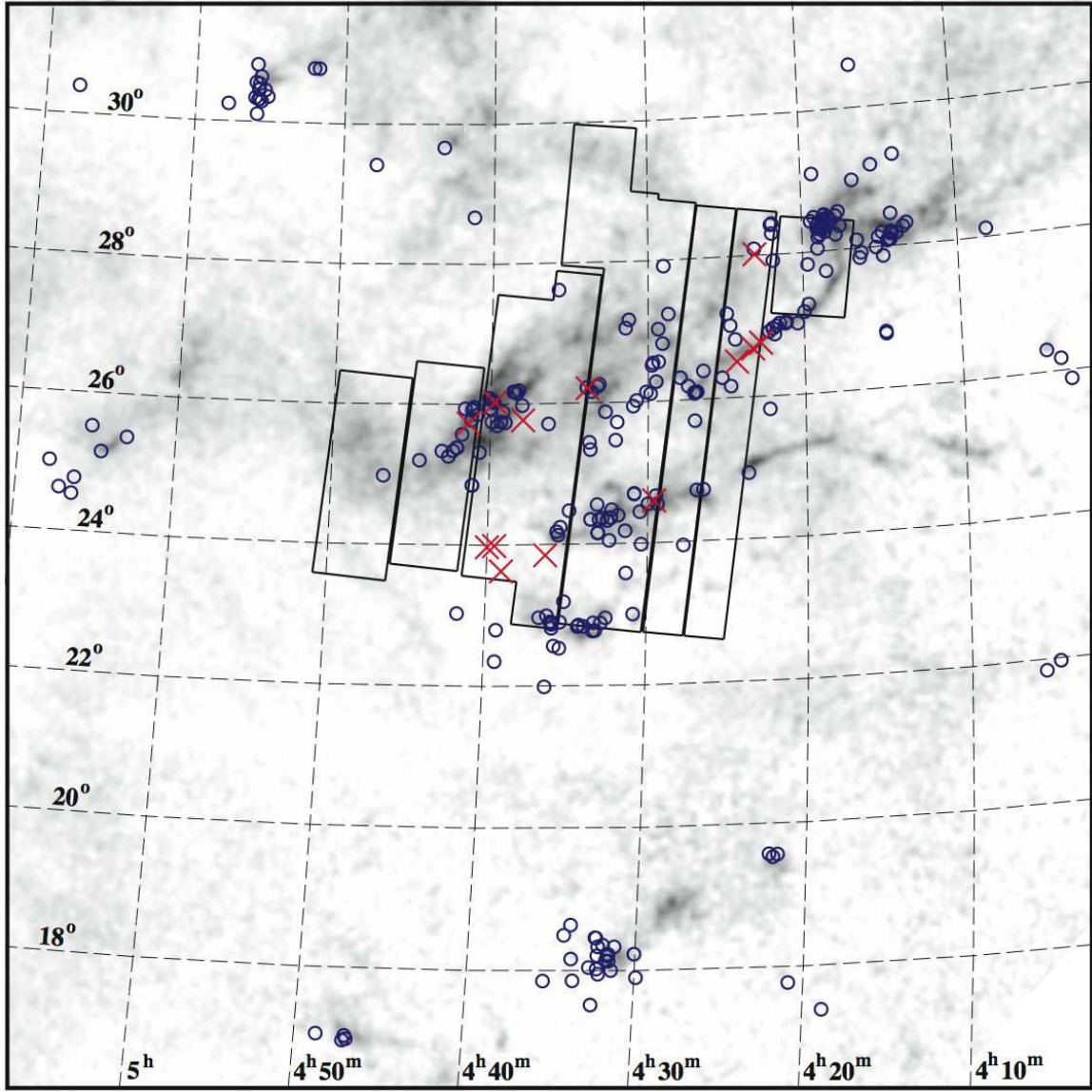


FIG. 1.— Spatial distribution of previously known members of the Taurus star-forming region (*circles*) and new members discovered in this work (*crosses*, Table 2) shown with a map of extinction (*grayscale*, Dobashi et al. 2005). The area imaged with IRAC aboard the *Spitzer Space Telescope* in this work is indicated (*solid lines*).

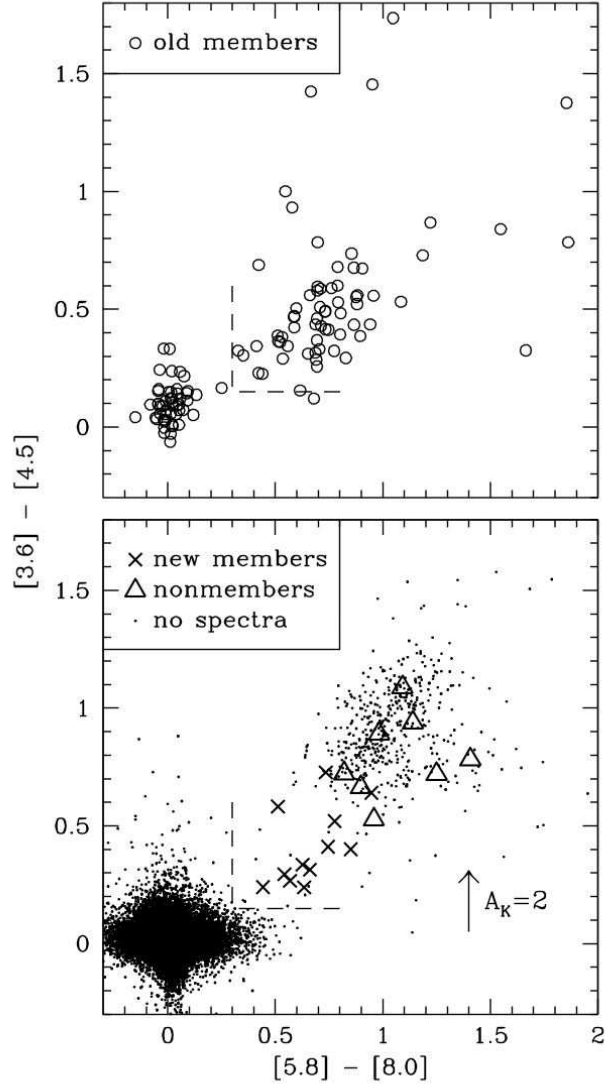


FIG. 2.— *Spitzer* IRAC color-color diagrams for the survey fields in the Taurus star-forming region indicated in Figure 1. *Top:* Among the previously known members of Taurus (circles, Table 4), the ones with circumstellar disks have colors of $[5.8] - [8.0] > 0.3$ and $[3.6] - [4.5] > 0.15$ (dashed line). *Bottom:* Among the other point sources in the survey, we obtained spectra of a sample of objects with colors in this diagram and magnitudes in Figure 3 that are similar to those of the known disk-bearing members of Taurus. The candidates classified as new members (crosses) and nonmembers (triangles) are listed in Tables 2 and 3, respectively. Only objects with photometric errors less than 0.1 mag in all four bands are shown in these two diagrams. The reddening vector is based on the extinction law from Indebetouw et al. (2005).

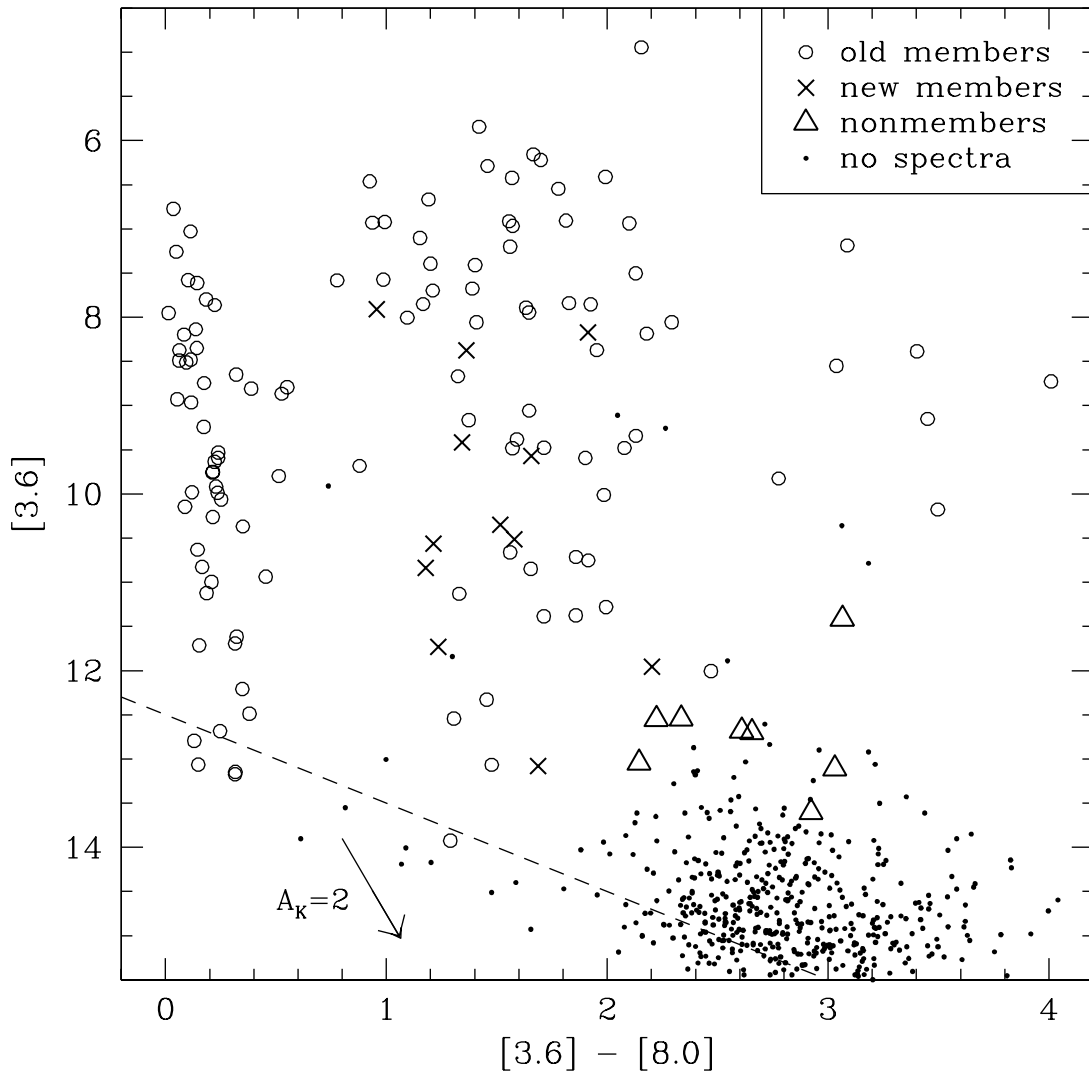


FIG. 3.— *Spitzer* IRAC color-magnitude diagram for the survey fields in the Taurus star-forming region indicated in Figure 1. We show the previously known members of Taurus in this survey area (*circles*) and a sample of new sources with colors in Figure 2 and magnitudes in this diagram that are similar to those of known disk-bearing members of Taurus, which we have spectroscopically classified as new members (*crosses*) and nonmembers (*triangles*). We also include the remaining sources from Figure 2 that have red colors ($[3.6] - [4.5] > 0.15$, $[5.8] - [8.0] > 0.3$) and lack spectroscopy (*points*). Only objects with photometric errors less than 0.1 mag in all four bands are shown in this diagram. The completeness limit for sources of this kind is shown (*dashed line*). The reddening vector is based on the extinction law from Indebetouw et al. (2005).

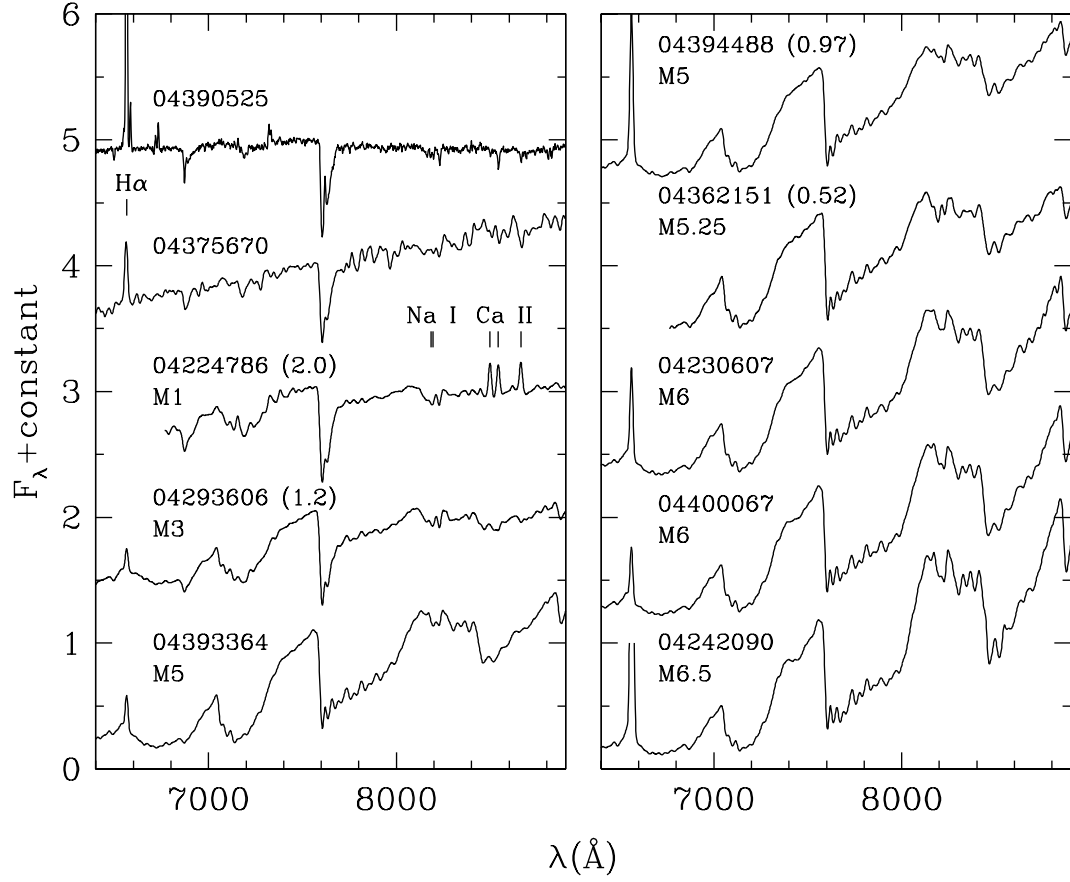


FIG. 4.— Optical spectra of new members of the Taurus star-forming region discovered in this work. Spectral types could not be measured from the data for the first two stars; the classifications for the remaining sources are indicated. The spectra of the M-type objects have been corrected for extinction, which is quantified in parentheses by the magnitude difference of the reddening between 0.6 and $0.9\ \mu\text{m}$ ($E(0.6 - 0.9)$). The spectrum of 2MASS 04390525+2337450 is shown at the observed resolution of $7\ \text{\AA}$ to facilitate the viewing of its emission lines. The remaining data are displayed at a resolution of $18\ \text{\AA}$. All data are normalized at $7500\ \text{\AA}$.

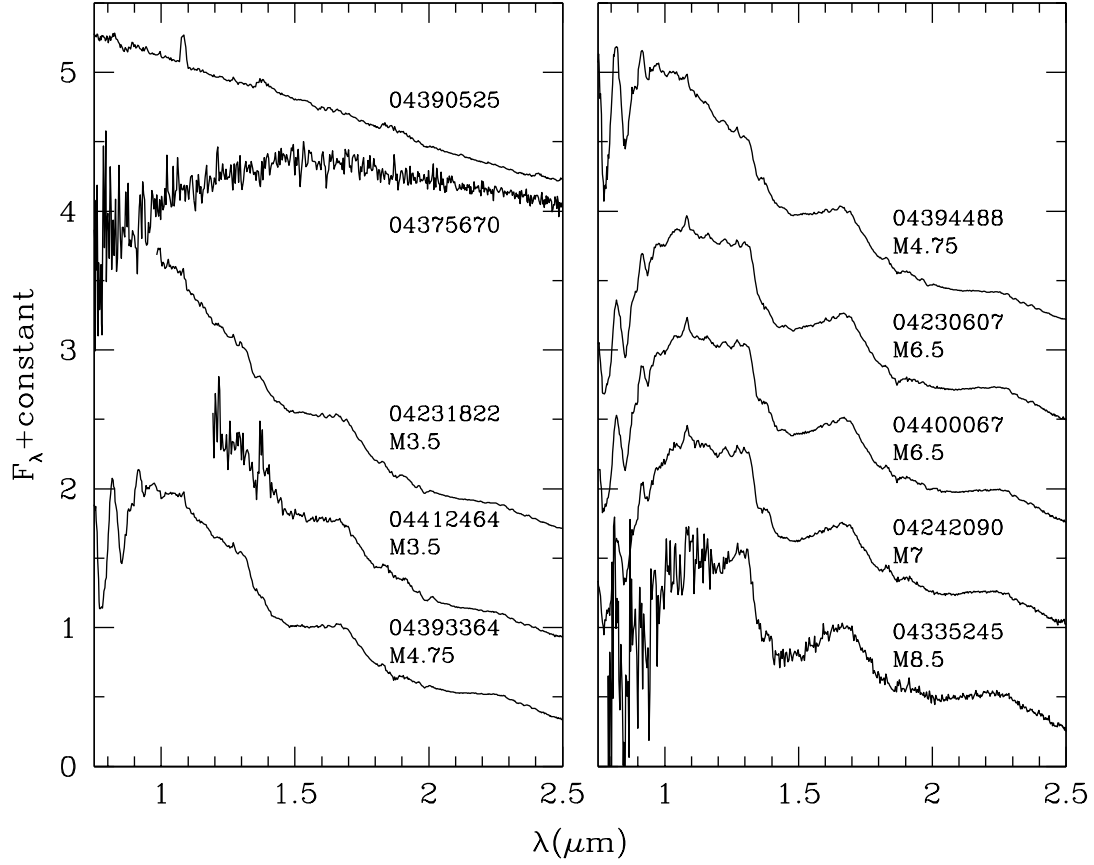


FIG. 5.— Near-IR spectra of new members of the Taurus star-forming region discovered in this work. Spectral types could not be measured from the data for the first two stars; the classifications for the remaining sources are indicated. The spectra for the M-type objects have been dereddened to the same slope as measured by the ratios of fluxes at 1.32 and 1.68 μm . These data have a resolution of $R = 100$ and are normalized at 1.68 μm .

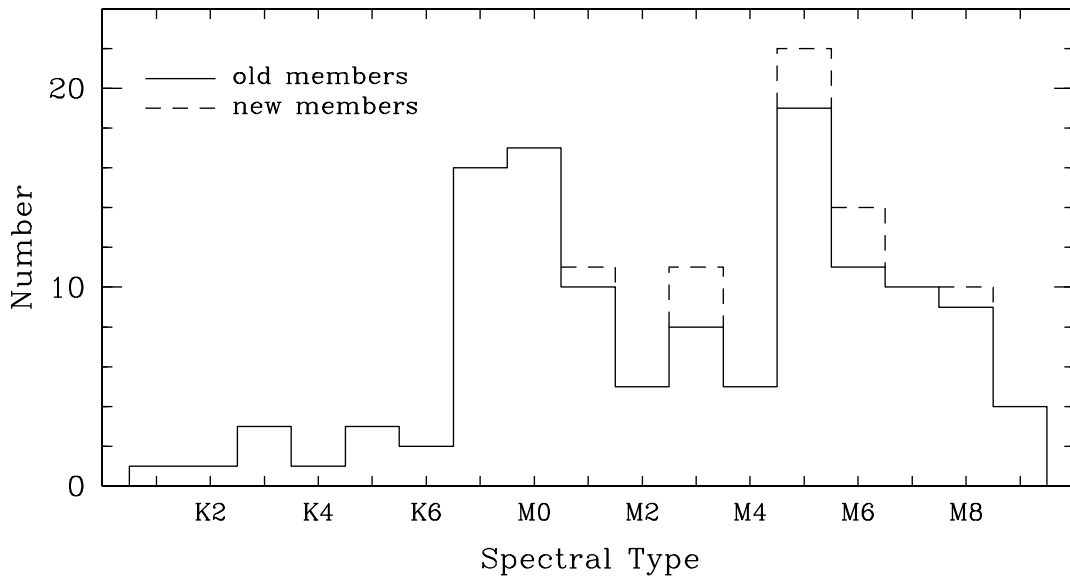


FIG. 6.— Distribution of spectral types for previously known members of the Taurus star-forming region within the survey field in Figure 1 (*solid histogram*) and the distribution after adding the new members discovered in this work (*dashed histogram*).